An Experimental Determination of the Cr−DMB (DMB = 3,3-Dimethyl-1-butene) Bond Energy in $Cr(CO)_5$(DMB): Effects of Alkyl Substitution on Chromium−Olefin Bond Energies in $Cr(CO)_5$(olefin) Complexes

David L. Cedeño[†] and Eric Weitz*

Department of Chemistry, Northwestern University, Evanston, Illinois 60208-3113

Received: October 22, 2001; In Final Form: February 25, 2002

The chromium−olefin complex $Cr(CO)_5$(DMB) (DMB = 3,3-dimethyl-1-butene) has been studied in the gas phase using transient infrared spectroscopy. This complex forms by addition of DMB to photogenerated $Cr(CO)_5$ with a rate constant, $k_L = (7.0 \pm 1.5) \times 10^{-11}$ cm^3 molecule^{-1} s^{-1}. The bond enthalpy for the DMB−$Cr(CO)_5$ bond has been determined from the kinetics for the decay of $Cr(CO)_5$(DMB) to be 20.1 ± 1.7 kcal/mol at 298 K. An energy decomposition analysis has been performed for a series of $Cr(CO)_5$(olefin) complexes (olefin = DMB, ethylene, propene, 1-butene, 1-hexene, *cis*-2-butene, *trans*-2-butene, isobutene, and tetramethylethylene (TME)) using density functional theory. These calculations provide insights into trends in the chromium−olefin bond energy. The results reveal that the trend in bond energies in these complexes correlates with the number and the nature of the alkyl groups around the double bond, and that the dominant factor in this trend is the deformation energy of the olefin and $Cr(CO)_5$, where the deformation energy is the energy required to deform the olefin ligand and the unsaturated metal centered moiety from their isolated ground-state geometries to the geometry they adopt in the bound complex.

I. Introduction

Metal−alkene complexes are of central importance in organometallic chemistry. They are involved in catalytic processes such as olefin isomerization, hydrogenation, and epoxidation.[1−4] Because these reactions involve the formation and/or cleavage of a metal−olefin bond, an understanding of metal−olefin interactions is necessary for the design of suitable catalysts for such processes. Since the early 1950s, the conventional description of the metal−olefin bond has been based on the Dewar−Chatt−Duncanson (DCD) model.[5,6] According to this model, the metal−olefin bond is the result of a synergistic contribution of two bonding interactions. The olefin's HOMO donates electron density to the metal centered-moiety's LUMO in a σ-type interaction, while the HOMO of the metal moiety donates electron density back to the olefin's empty π^* LUMO through a π-type interaction, referred to as back-bonding. In terms of the DCD model, the interactions of substituted olefins and a common metal fragment are influenced by the substituents around the C=C bond because these substituents affect the electron donating and accepting capabilities of the olefin ligand.[2,7] For instance, if the electronegativity of the olefin's substituents is increased, the olefin becomes more electron withdrawing, and the π-type interaction would be favored (bearing in mind that the olefin's electron donating capability could also be affected). On the other hand, electron-donating substituents should enhance σ-type interactions (although back-bonding could also be affected). Alkyl groups (i.e., methyl, ethyl, *tert*-butyl, etc.) are typically considered to be electron donating substituents, implying that alkyl substituted olefins would be expected to have a stronger σ interaction than ethylene. In terms of this picture, the greater the number of alkyl groups around the double bond the stronger the metal−olefin interaction should be. However, it is well-known that increasing the number (and size) of alkyl groups around the double bond also increases the steric interaction between the olefin and the other ligands bound to the metal.[8−10] The net effect of this is a metal−olefin interaction which is *weaker* than that for a less substituted olefin. The focus of this paper is to analyze, in detail, the metal−olefin bonding interactions in a series of chromium pentacarbonyl−olefin complexes in order to determine how the strength and nature of the metal−olefin bond is affected by alkyl groups around the C=C bond. Since there is available experimental[10,11] data on bond energies (BDE) for olefin = ethene (Eth), propene (Pro), 1-butene (But), *cis*-2-butene (c-2-but), *trans*-2-butene (t-2-but), isobutene (isobut), 1-hexene (Hex), and tetramethylethylene (TME), the results of calculations on these complexes can be compared to available data.

McNamara et al.[10] determined that, in the complexes they studied (olefin = Eth, Pro, But, c-2-but, t-2-but, isobut, and 2-methyl-2-butene) the rate of dissociative loss of the olefin increases with the length of the alkyl chain and the number of substitutents, due to an increase in the preexponential, while the chromium−olefin bond energy is basically unaffected. Yang et al.[11] found that the Cr−TME BDE in $Cr(CO)_5$(TME) is smaller than the Cr−Hex BDE in $Cr(CO)_5$(Hex), suggesting that the number of alkyl moieties around the double bond affects the metal−alkyl BDEs. Here we provide an experimental determination of the Cr−DMB BDE in $Cr(CO)_5$(DMB) (DMB = 3,3-dimethyl-1-butene). DMB has been chosen because it is similar to ethylene except that a "bulky" *tert*-butyl group substitutes for one of the hydrogens of ethylene. On the basis of prior work,[12] we hypothesize that the presence of a *tert*-butyl substituent should lead to repulsive interactions which are expected to reduce the Cr−DMB BDE relative to the chromium−ethylene BDE in $Cr(CO)_5(C_2H_4)$.

[†] Present address: Department of Chemistry, Illinois State University, Normal, IL 61790.

10.1021/jp013912b CCC: $22.00
Published on Web 04/17/2002

To gain more detailed insights into bonding interactions in these complexes we have performed density functional theory (DFT) calculations to decompose the calculated chromium−olefin bond energies into terms that can be attributed to attractive and repulsive orbital interactions, and to the energy necessary to deform the olefin and the $Cr(CO)_5$ moiety from their ground-state equilibrium geometries to the ones they adopt in the bound complex. The results of the bond energy decomposition analysis, as well as the changes in Mulliken populations of the frontier molecular orbitals (FMO) of the olefin, provide insights into the relative importance of various factors that can affect the magnitude of the olefin−metal BDE: attractive electronic interactions (σ-donation and back-donation), steric interactions and deformations of the olefin and of $Cr(CO)_5$.

II. Experimental Section

The experimental setup used to determine gas-phase metal−ligand bond energies has been described in detail elsewhere.[13] A brief description is provided here for convenience. Gas-phase $Cr(CO)_6$ (0.05−0.06 Torr), CO (1.0−46 Torr), and 3,3-dimethyl-1-butene (DMB, 45−100 Torr) are introduced into a 42 cm water-jacketed Pyrex glass cell terminated by CaF_2 windows. Photolysis of $Cr(CO)_6$ is accomplished using the output of a frequency-tripled Nd:YAG laser at 355 nm with a fluence of $\sim$6−7 mJ/cm^2 at the cell window. Since $Cr(CO)_5$ is produced almost exclusively when $Cr(CO)_6$ is irradiated with 351 nm light,[14] and the degree of unsaturation of gas phase photoproducts generally decreases with an increase in photolysis wavelength,[15] $Cr(CO)_5$ would be expected to be an even more predominant photoproduct when $Cr(CO)_6$ is photolyzed at 355 nm. The experiment is initiated by photolysis of the gas-phase sample for 35 s at a laser frequency of 10 Hz. The rise and decay of reaction products formed at different DMB and CO pressures ratios were monitored using a FTIR spectrophotometer operating in the GC mode over the 1900−2200 cm^{-1} range. A liquid N_2-cooled InSb detector was used to detect the infrared beam. Temperature control was achieved using a constant-temperature bath, which circulated water through the cell jacket. The temperature, monitored by a chromel−alumel thermocouple, was varied over the range from 279 to 298 K with an uncertainty of $\pm$1 K.

A different experimental setup[13] was used to determine the rate constant (k_L) for addition of DMB to $Cr(CO)_5$. This rate constant is necessary in order to obtain the rate constant, (k_d), for olefin dissociation. In these experiments $Cr(CO)_6$ (0.04−0.05 Torr) was photolyzed with the 308 nm output of an excimer laser operating on XeCl at a fluence of $\sim$ 6−7 mJ/cm^2 at the cell window. With 308 nm photolysis radiation a mixture of $Cr(CO)_4$ and $Cr(CO)_5$ is obtained.[15] The addition of CO and buffer gas to the cell lead to a larger effective yield of $Cr(CO)_5$ relative to $Cr(CO)_4$. A liquid N_2-cooled IR diode laser was used to probe the decay rate of $Cr(CO)_5$ at 1978 cm^{-1} and the rise rate of $Cr(CO)_5$(DMB) at 1958 cm^{-1} as a function of added DMB (0−0.7 Torr). Sufficient helium (>35 Torr) was added to the photolysis cell in order to ensure that the rate measurements are in the "high-pressure limit".[13] A fast response ($\sim$250 ns) liquid N_2-cooled InSb detector monitored the intensity of the IR laser probe. This signal was amplified ($\times$100) and fed to a digital storage oscilloscope and the average of at least 10 laser pulses was send to a computer for analysis.

$Cr(CO)_6$ (Strem Chemicals) and DMB (>95% Aldrich) were subjected to at least three freeze−pump−thaw cycles prior to usage. CO (99.9% Matheson) and Helium (99.999%, Praxair) were used as received.

III. Computational Details

Equilibrium geometries for $Cr(CO)_5$(olefin) (olefin = ethylene, propene, 1-butene, 1-hexene, DMB, *cis*-2-butene, *trans*-2-butene, isobutene, and tetramethylethylene) were calculated with the Jaguar[16] quantum chemistry program. All calculations were performed using density functional theory (DFT) and the local density approximation (LDA) of Vosko et al. (VWN).[17] Nonlocal density functionals were added self-consistently. Becke's[18] was used for exchange and Perdew's[19] for correlation. The LACVP** basis set and the frozen core approximation were used. LACVP** uses Hay and Wadt's effective core potential (ECP)[20] basis set for metals, in which the outermost core orbitals are included. For nonmetal atoms, LACVP** employs the 6-31G** basis set.[21]

Bond energies (ΔE_c) were calculated from the difference in the optimized energies (E_c) of the singlet ground states of the products and the reactants for the reaction:

$$Cr(CO)_5(\text{olefin}) \rightarrow Cr(CO)_5 + \text{olefin} \quad (1)$$

$$\Delta E_c = E_c[Cr(CO)_5] + E_c[\text{olefin}] - E_c[Cr(CO)_5(\text{olefin})] \quad (2)$$

This energy, ΔE_c, is the reaction energy for olefin dissociation. Thus, by definition, *factors that lead to an increase in bonding interactions are positive*.

The bond enthalpy at 298 K is calculated from ΔE_c using the following algebraic expression:[22]

$$\Delta H_c = \Delta E_c + \Delta ZPE + \Delta E_{th} + \Delta(PV) \quad (3)$$

where ΔZPE is the zero point energy correction obtained from an unscaled calculation of the vibrational frequencies; ΔE_{th} is the change associated with the translational, rotational and vibrational energy in going from 0 to 298 K; and $\Delta(PV)$ is the molar work which, using an ideal gas approximation, is equal to ΔnRT. As with other metal−olefin systems we have treated, better agreement between calculations and experiment is obtained without inclusion of the basis set superposition error correction. This is discussed in more detail in ref 23.

Bond energy decomposition analyses were performed using the Amsterdam Density Functional program (ADF2000).[24] The decomposition analysis is based on an extended transition state method.[25,26] All energy decomposition analyses were performed using the same BP86 functional employed for geometry optimization. However, when using ADF, the atomic orbitals on chromium were described by an uncontracted triple-ζ STO basis set,[27] while a double-ζ STO basis set was used for hydrogen, carbon, and oxygen. A single-ζ polarization function and the frozen core approximation[24b] were used for all atoms (except hydrogen). A set of auxiliary s, p, d, f, g, and h STO functions, centered on all nuclei, was used in order to fit the molecular density and represent the Coulomb and exchange potentials accurately in each SCF cycle.[28]

The bond energy can be decomposed into contributions from three terms:

$$\Delta E_c = \Delta E_{oi} + \Delta E_{steric} + \Delta E_{def} \quad (4)$$

The deformation energy (ΔE_{def}) is the energy necessary to transform the bonding moieties from their respective isolated equilibrium geometries to the geometries they assume in the bound complex. The steric energy (ΔE_{steric}) is the sum of two terms, one corresponding to the electrostatic interaction (ΔE_{elst}) between the fragments, and the other to the Pauli repulsion energy (ΔE_{pauli}), which dominates the steric term. The orbital

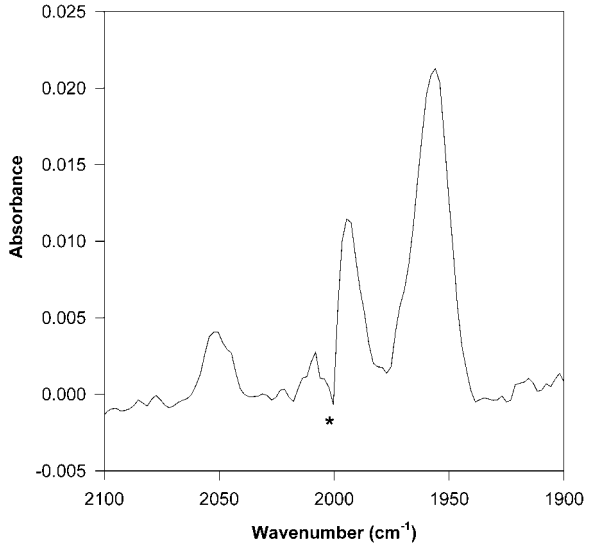

Figure 1. The FTIR spectrum of $Cr(CO)_5$(DMB) obtained 5 s after 355 nm photolysis of a mixture containing 0.050 Torr $Cr(CO)_6$, 1 Torr CO, and 50 Torr DMB. A scaled $Cr(CO)_6$ spectrum has been subtracted to account for photolytic depletion of parent ("*" denotes incomplete subtraction in the region of parent absorption).

interaction energy (ΔE_{oi}) is the energy due to the interactions between occupied orbitals of one fragment and empty orbitals of the other fragment, as well as between the occupied and empty orbitals within a given fragment (polarization). The sum of ΔE_{oi} and ΔE_{steric} represents the total attractive electronic interaction energy (In our terminology this is ΔE_{int}, which is the quantity that is sometimes referred to as the "bond-snap" energy). Additionally, a Mulliken population analysis[29] was performed for each system to evaluate population changes occurring when a ligand and a metal fragment interact. When comparing one complex to another, in the context of the experimental and calculated data, some of the energy differences are within the experimental and calculational error limits. However, we focus on a comparison of *trends* in experimental and calculated bond energies, and the contributions of various factors to these bond energies and the trend in bond energies.

IV. Results

A. Experimental Determination of the Chromium−DMB Bond Enthalpy. Figure 1 shows the FTIR spectrum of $Cr(CO)_5$(DMB) obtained 5 s after 355 nm photolysis (350 shots) of a mixture containing a 50:1 DMB/CO pressure ratio. The spectrum of $Cr(CO)_6$ has been subtracted out to compensate for its photolytic depletion. The absorptions at 1957 and 2051 cm^{-1} have the same kinetic behavior, as would be expected for two absorptions belonging to the same species. There is also a band in the 2000 cm^{-1} region, which is not well resolved due to the effects of the subtraction of the strong $Cr(CO)_6$ absorption in this region. Comparison with spectroscopic data for other chromium pentacarbonyl−olefin complexes in the gas phase[10] are consistent with these absorptions being assigned to $Cr(CO)_5$(DMB). Additional evidence that these bands correspond to $Cr(CO)_5$(DMB) absorptions is given by the fact that the rate of appearance of the species at 1957 cm^{-1} is proportional to the DMB pressure, and matches the rate of decay of $Cr(CO)_5$. The rate constant for addition of DMB to $Cr(CO)_5$ (k_L) was obtained from the dependence of both the decay rate of $Cr(CO)_5$ and the rise rate of $Cr(CO)_5$(DMB), as a function of the DMB pressure. A value of $(6.7 \pm 1.0) \times 10^{-11}$ cm^3 $molecule^{-1}$ s^{-1} was obtained from the decay of $Cr(CO)_5$ monitored at 1979 cm^{-1}, and a value of $(7.6 \pm 2.7) \times 10^{-11}$ cm^3 $molecule^{-1}$ s^{-1} from the rise of product at 1958 cm^{-1}. A weighed average value of $(7.0 \pm 1.5) \times 10^{-11}$ cm^3 $molecule^{-1}$ s^{-1} is obtained for k_L at 297 K. Within experimental error, k_L is temperature independent over the range from 279 to 298 K.

Dissociative loss of a weakly bound ligand is expected, especially when "ligand slippage" processes, which can open up a site in the coordination sphere of the metal are effectively precluded. Without ligand slippage an associative substitution process would require a greater than 18 electron intermediate. This is an unlikely occurrence in this system since the relevant ligand association processes are unactivated. The kinetic mechanism, which is predicated on dissociative ligand loss, that is used to determine k_d, the rate constant for loss of DMB from $Cr(CO)_5$(DMB), is outlined in eqs 5−7:

$$Cr(CO)_5(DMB) \rightarrow Cr(CO)_5 + DMB \; k_d \qquad (5)$$

$$Cr(CO)_5 + DMB \rightarrow Cr(CO)_5(DMB) \; k_L \qquad (6)$$

$$Cr(CO)_5 + CO \rightarrow Cr(CO)_6 \; k_{CO} \qquad (7)$$

In this reaction sequence, the phenomenological rate of regeneration of $Cr(CO)_6$, k_{obs}, (see eq 8) is limited by the rate of loss of olefin (eq 5) while the rate of regeneration of $Cr(CO)_6$ is the same as the rate of decay of $Cr(CO)_5$(DMB). Applying the steady-state approximation to $Cr(CO)_5$, the observed phenomenological decay rate (k_{obs}) is given by

$$k_{obs} = k_d k_{CO}[CO]/\{k_L[DMB] + k_{CO}[CO]\} \qquad (8)$$

which can be rewritten as

$$k_d = k_{obs}\left\{1 + \frac{k_L}{k_{CO}}\frac{[DMB]}{[CO]}\right\} \qquad (9)$$

$Cr(CO)_5$(DMB) decay rates were measured at 1956 cm^{-1}, for different DMB/CO ratios. In addition, in a few runs, common C_2Cl_4/CO pressure ratios were obtained by varying the individual ligand pressures; in all cases k_{obs} depended on the pressure ratio, not the individual pressures. As expected for the dissociative mechanism shown in eqs 5−7 there is recovery of $Cr(CO)_6$, and the decay of $Cr(CO)_5$(DMB) gets faster as the DMB/CO ratio is decreased. The rate constant for dissociative loss of olefin (k_d) can be obtained from k_{obs}, if the DMB/CO pressure ratio and the addition rate constants, k_{CO} and k_L, are known. k_{CO} has been previously determined.[14,30−34] A rough determination of k_{CO} from the intercept of the DMB dependent plots agrees best with the value of 2.5×10^{-11} cm^3 $molecule^{-1}$ s^{-1} reported by Seder et al.[14,31] Within the experimental error, k_{CO} has been found to be temperature independent in the temperature range of relevance to the present experiments.

The activation energy (E_a) and preexponential (ln A) for k_d are obtained from the Arrhenius plot shown in Figure 2. From the slope of this plot, $E_a = 19.5 \pm 1.7$ kcal/mol and from the intercept, ln $A = 32.7 \pm 3.0$. Since the association of DMB with $Cr(CO)_5$ is unactivated, the bond dissociation enthalpy for the Cr−DMB bond is directly related to the activation energy,[13] and is determined to be 20.1 ± 1.7 kcal/mol at 298 K.

Table 1 summarizes the available experimental BDEs for different chromium pentacarbonyl olefin complexes.

B. Calculated Chromium−Olefin Bond Energies. Table 1 also shows the calculated values for ΔE_c and ΔH_c^{298}. Note that the calculated bond energies (and enthalpies) follow a rather smooth trend and, in general, *decrease* as the number of alkyl

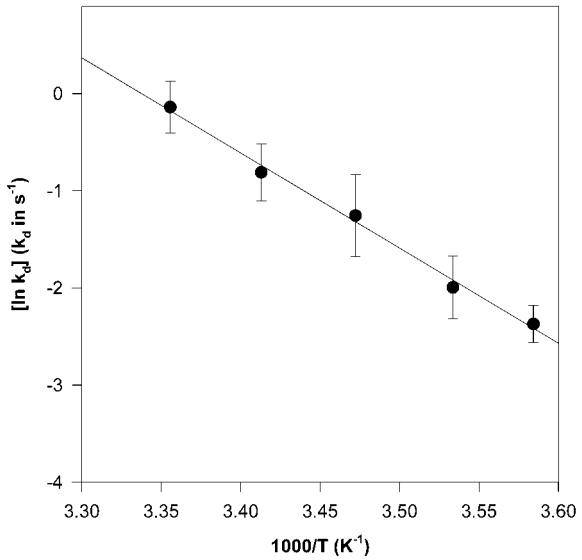

Figure 2. An Arrhenius plot for the rate constant for dissociative loss of olefin from $Cr(CO)_5$(DMB) (k_d in s^{-1}) over the 279−298 K range.

TABLE 1: Calculated and Experimental Bond Energies and Enthalpies, and Experimentally Determined Preexponentials for Chromium−Olefin Bond Dissociation in $Cr(CO)_5$(olefin) Complexes[a]

olefin	ΔE_c	ΔZPE	$\Delta E_{th} + \Delta(PV)$	ΔH_c	ΔH_{exp} or ΔE_{exp}[b]	ln *A*
ethene	26.4	−3.2	0.6	23.8	25.1 ± 1.0[c]	38.4 ± 0.9
					24.0 ± 0.3[d]	38.2 ± 0.2
					24.7 ± 2.4[e]	37.3 ± 4.0
Monoalkyl Ethylenes						
propene	24.2	−1.4	0.2	23.0	24.2 ± 0.3[d]	39.8 ± 0.2
butene	24.5	−4.4	0.3	20.4	24.2 ± 0.3[d]	40.5 ± 0.3
hexene	25.3	−5.2	0.8	20.9	22.2 ± 2.4[f]	- - - -
DMB	20.0	−1.0	−0.4	18.6	20.1 ± 1.7[g]	32.7 ± 3.0
Dialkyl Ethylenes						
cis-2-butene	22.9	−4.5	1.0	19.4	24.8 ± 0.3[d]	41.4 ± 0.5
trans-2-butene	21.6	−3.8	0.9	18.7	24.6 ± 0.3[d]	42.8 ± 0.4
iso-butene	21.8	−0.5	−0.3	21.0	24.1 ± 0.3[d]	42.1 ± 0.3
Tetraalkyl Ethylenes						
TME	17.9	−2.9	0.5	15.5	19.6 ± 2.4[f]	

[a] Energies in kcal/mol, preexponential, *A*, in s^{-1}. [b] Values are for ΔH at 298 K except for those as indicated in the footnote. [c] Gas phase, from ref 38, given as ΔE at 298 K. [d] Gas phase, from ref 10, given as ΔE at 298 K. [e] Gas phase, from ref 30. [f] In heptane solution from ref 11. [g] This work.

groups around the C═C bond *increase*. For example, the trend for the chromium−olefin bond energy (ΔE_c) is Eth > Hex > Pro, But > c-2-but > t-2-but, iso-but > DMB > TME. In general ΔE_c for the monoalkyl olefin complexes is larger than ΔE_c for the dialkyl and tetraalkyl olefin complexes. The exception is the DMB complex which has a ΔE_c that is ∼4−5 kcal/mol lower than ΔE_c's for the other monoalkyl substituted olefins (ethylene, propene, butene, and hexene: i.e., R−CH═CH_2) complexes. When the calculated bond enthalpies (ΔH_c) are considered, the trend changes, somewhat, to Eth > Pro > iso-but, Hex > But > c-2-but > t-2-but, DMB > TME. The difference between the trends in ΔE_c and ΔH_c is due to the differences in the calculated ΔZPE and the vibrational energy of each complex (see eq 4). Because both of these terms are obtained from the calculated vibrational frequencies, the uncertainty in the determination of these frequencies is reflected in the ΔZPE and the vibrational energy, and thus in the enthalpy. The total uncertainty for ΔZPE and the vibrational energy (∼2−3 kcal/mol) is of the same magnitude as the difference

CHART 1

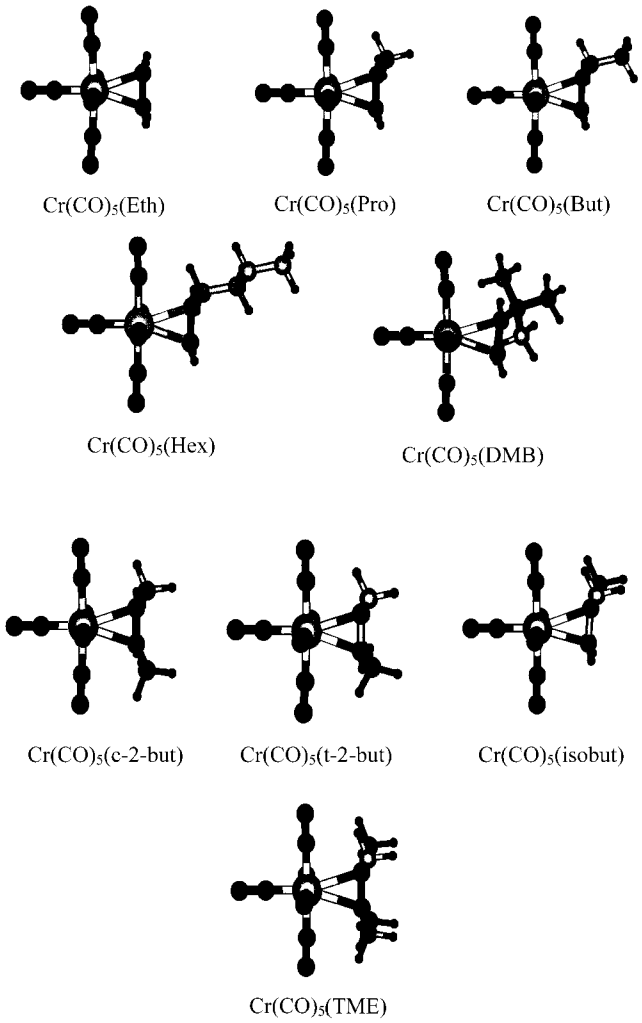

between the ΔE_c values of some of the complexes. However, independent of these differences between ΔE_c and ΔH_c, our calculations indicate that the number and size of the alkyl groups around the C═C bond affects the chromium−olefin bond strength.

C. Calculated Geometries. Chart 1 shows the calculated equilibrium geometries for the complexes under study. The relevant data are summarized in Table 2. Table 3 shows the calculated geometrical data for the free olefins and for $Cr(CO)_5$. To our knowledge, there are no experimental structural data on the complexes in Chart 1. However, there is an X-ray structure for a related complex: $Cr(CO)_5$(endo-6-arylbicyclo[3.1.0]hex-2-ene).[35] This bicycloolefin is a disubstituted ethylene (RHC═CHR′), and like *cis*-2-butene the two alkyl groups are in a cis configuration (see Chart 2). A comparison between the available data for this complex and calculated data is thus possible. The average experimental Cr−C(olefin) bond length in this complex is 2.393 Å, which is very close to the value for Cr−C(olefin) bond in *cis*-2-butene (2.412 Å). The experimental C═C bond length is shorter than the calculated values by ∼0.03 Å. Also, the trend in the Cr−C(O) bond lengths in $Cr(CO)_5$(endo-6-arylbicyclo[3.1.0]hex-2-ene) is well reproduced by the calculations: $Cr-C_{trans} < Cr-C_{eq} < Cr-C_{ax}$. The experimental $Cr-C_{trans}$ value of 1.849 Å is very close to the calculated values, which are in the range 1.839−1.850 Å. Furthermore, the calculated $Cr-C_{eq}$ and $Cr-C_{ax}$ bond lengths do not differ significantly from the experimental values (1.888 and 1.923 Å respectively), although the relative difference between the

TABLE 2: Calculated Geometrical Parameters for $Cr(CO)_5$(olefin) Complexes[a]

	Eth	Pro	But	Hex	DMB	c-2-but	t-2-but	isobut	TME
$Cr-C_{ol}$	2.323	2.332	2.332	2.332	2.369			2.357	
		2.403	2.396	2.398	2.492	2.412	2.396	2.532	2.492
$Cr-C_{tr}$	1.850	1.846	1.845	1.846	1.839	1.842	1.844	1.842	1.839
$Cr-C_{ax}$	1.887	1.886	1.886	1.887	1.888	1.887			
		1.886	1.886	1.886	1.885	1.883	1.886	1.884	1.884
$Cr-C_{eq}$	1.887	1.888	1.887	1.887	1.888	1.882		1.890	
		1.883	1.882	1.882	1.885	1.882	1.883	1.876	1.880
C═C	1.389	1.390	1.391	1.390	1.384	1.393	1.393	1.390	1.404
$C-C_{alk}$		1.508	1.513	1.511	1.531	1.509	1.509	1.514	1.520
$C-Cr-C_{ax}$[c]	178.4	178.0	178.8	179.2	183.1	178.4	179.7	178.4	181.6
$C-Cr-C_{eq}$[c]	183.7	184.0	183.6	183.3	184.1	184.0	183.4	183.2	182.0
$Cr-C-O_{ax}$	179.6	179.3	179.6	179.5	177.9	179.5			
		178.8	178.9	178.4	174.7	178.3	178.2	178.8	177.7
$Cr-C-O_{eq}$	179.5	179.2	179.4	179.5	179.3	178.9		179.5	
		178.7	178.9	179.1	175.7	178.9	179.0	178.5	179.1
R−C−H		115.7	115.4	115.6	113.6	115.2	115.4		
R−C−R								114.8	111.8
H−C−H	116.0	116.1	116.1	116.1	115.9			116.2	
Θ_{HH}[b]	21.1	17.8	18.4	18.2	14.5		15.1		
Θ_{RH}[b]		27.2	28.3	27.8	32.4	23.4		22.8	
Θ_{RR}							36.7		28.2

[a] Bond lengths in angstroms, angles in degrees. Unless indicated in the row entry, value in the first line of a cell is relative to H position in the olefin, and the second line is relative to the alkyl group position. Subscripts: tr = CO trans to olefin, ax = CO cis to olefin and perpendicular to C═C, eq = CO cis to olefin and parallel to C═C. [b] Θ is the angular deviation of substituents from the plane containing the C═C bond (Θ = 180-dihedral angle: Θ_{HH} for H−C═C−H, Θ_{RH} for R−C═C−H, and Θ_{RR} for R−C═C−R, R = alkyl). [c] Values of >180° indicate bending of CO ligands "away" from the olefin.

TABLE 3: Calculated Geometries[a] for the Ground State of $Cr(CO)_5$ (C_{4v}) and the Relevant Olefins

$Cr(CO)_5$						
$Cr-C_{pl}$	$Cr-C_{\perp}$	$C-O_{pl}$	$C-O_{\perp}$	$C_{pl}-Cr-C_{pl}$	$Cr-C-O_{pl}$	$Cr-C-O_{\perp}$
1.894	1.814	1.164	1.170	178.6	178.9	180.0

Free Olefins

	Eth	Pro	But	Hex	DMB	c-2-but	t-2-but	isobut	TME
C═C	1.338	1.342	1.342	1.341	1.341	1.347	1.344	1.345	1.356
$C-C_{alk}$		1.502	1.504	1.504	1.519	1.503	1.502	1.509	1.511
H−C−H	116.4	116.7	116.7	116.7	116.5			116.9	
R−C−H		116.1	115.7	115.8	114.0	115.2	116.4		
R−C−R								115.8	110.8

[a] Bond lengths in angstroms, angles in degrees; subscript pl refers to the 4 COs positioned in the molecular plane containing the metal, and ⊥ to the CO perpendicular to that plane, along the C_4 symmetry axis.

CHART 2

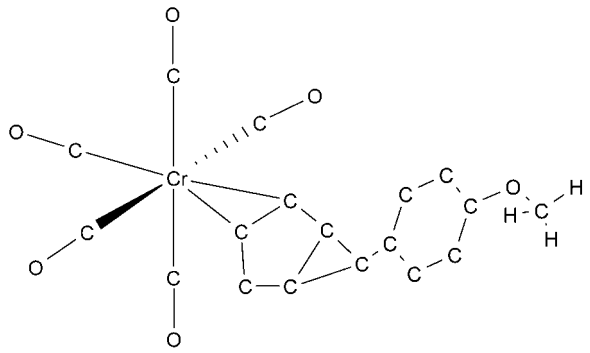

experimental $Cr-C_{ax}$ and $Cr-C_{eq}$ bond lengths is larger than the calculated one. In agreement with experimental data, the calculated $C_{eq}-Cr-C_{eq}$ angle is larger than the $C_{ax}-Cr-C_{ax}$ angle. We take the good agreement between the experimental data and the calculations for the $Cr(CO)_5$(endo-6-arylbicyclo-[3.1.0]hex-2-ene) complex as an indication of the accuracy of the DFT method for geometrical data for such complexes and feel this agreement is an indicator of the reliability of the calculations for the $Cr(CO)_5$(olefin) complexes.

V. Discussion

A. Electronic Orbital Interactions. An energy decomposition analysis of the chromium−olefin bond energies was performed, (as per eq 4), to obtain more insights into trends in the calculated bond energies. The results are shown in Table 4. The decomposition analyses reveal trends that are quite interesting in the context of the conventional view of the effect of alkyl substitution on the metal−olefin bond energy in a metal−olefin complex. Although it has been recognized that steric effects are an important factor in the stability of metal−olefin complexes, "conventional wisdom" is that alkyl substitution around the double bond should increase the σ-donating capability of an olefin.[36] The expectation, in terms of the qualitative picture of the DCD model, is that the increased σ-interaction should lead to stronger metal−olefin electronic interactions.[5,6,36] As shown in Figure 3, as the number of alkyl groups around the C═C bond increases, the energy of the HOMO of the substituted olefins increases relative to the HOMO energy of ethylene. With everything else being equal, the smaller the olefin HOMO−metal LUMO energy gap the better the olefin is at donating electron density. Therefore, TME, which has the smallest energy gap, might be expected to interact most strongly via σ-donation with $Cr(CO)_5$, while ethylene, which has the largest gap might

TABLE 4: Energy Decomposition Results for $Cr(CO)_5$(olefin) Complexes

	Eth	Pro	But	Hex	DMB	c-2-but	t-2-but	isobut	TME
ΔE_{pauli}	−103.9	−97.3	−98.2	−98.3	−86.4	−90.5	−94.3	−85.4	−78.7
ΔE_{elst}	77.7	75.6	76.3	76.3	67.6	72.9	75.6	68.5	66.2
ΔE_{steric}	−26.2	−21.7	−21.9	−22.0	−18.8	−17.6	−18.7	−16.9	−12.5
ΔE_{oi}	59.4	55.0	55.7	55.7	49.0	51.1	53.3	48.6	45.4
ΔE_{int}	33.2	33.3	33.8	33.7	30.2	33.5	34.6	31.7	32.9
ΔE_{def} olefin	−5.6	−6.5	−6.7	−6.5	−7.6	−6.8	−9.1	−6.5	−8.8
ΔE_{def} metal	−1.1	−2.6	−2.6	−2.6	−2.6	−3.8	−3.9	−3.4	−6.2
ΔE_c	26.5	24.2	24.5	24.6	20.0	22.9	21.6	21.8	17.9

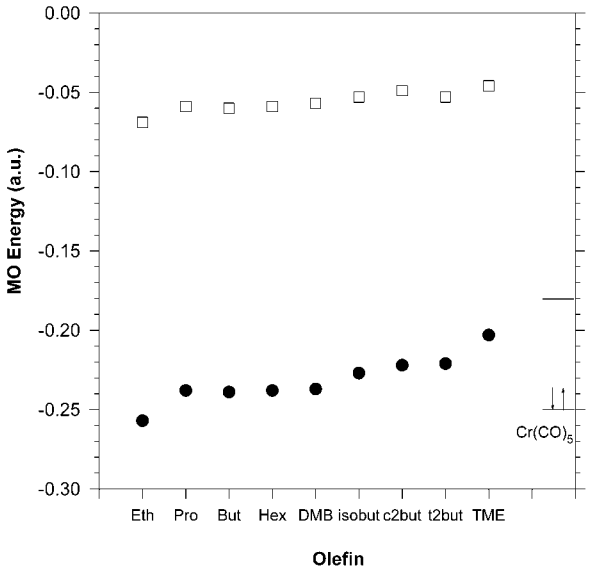

Figure 3. A DFT calculation of the HOMO (●) and LUMO (□) energies of olefins relative to the HOMO and LUMO energies of $Cr(CO)_5$.

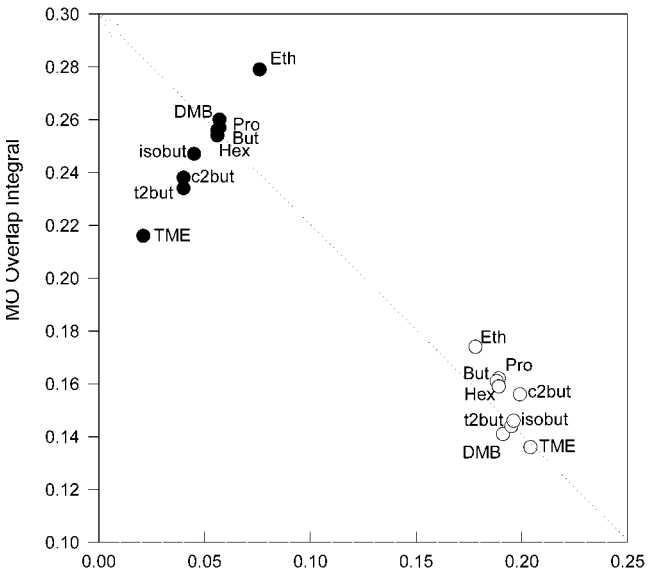

Figure 4. A graph displaying the metal−ligand overlap integral and the FMO energy gaps. Circles (●) are for the σ donation interaction, and open circles (○) for the back-bonding interaction. Qualitatively bonding capabilities increase for each bonding modality along the diagonal from the lower right corner to the upper left corner.

be expected to have the weakest σ interaction. The increase in σ donation should lead to a stronger metal−olefin interaction. However, everything else is not equal. The attractive orbital interaction energy (ΔE_{oi}) term in the energy decomposition analysis shows the opposite trend: that is, *an increase in the number of alkyl groups around the double bond does not lead to a stronger attractive electronic interaction*. This is principally a result of two factors. One factor is related to the effect of the interaction between the olefin LUMO and the metal fragment HOMO on the "back-bonding interaction" in these complexes. As seen in Figure 3, the olefin LUMO energy also increases somewhat with the number of alkyl groups around the C═C bond. This change leads to a larger metal HOMO−olefin LUMO gap for back-bonding, thus decreasing the effective π interaction. The second factor is the effect of the alkyl substituents on orbital overlap. The bonding interactions of a ligand depend on both the HOMO−LUMO energy gap, and the overlaps of the MOs involved in both σ and π metal−olefin interactions. To help illustrate the qualitative effects of both energy gaps and overlaps on the metal−olefin interactions a graph depicting "bonding capability" (Figure 4) has been constructed. In this graph, the HOMO−LUMO energy gaps are plotted on the abscissa and the magnitude of the normalized HOMO−LUMO overlap integrals are plotted on the ordinate. Stronger interactions are expected for small energy gaps *and* larger MO overlaps. Bonding capabilities for each bonding modality (σ and π) increase along the diagonal going from the bottom right corner to the upper left corner of the graph.

The implications of the bonding capability graph (Figure 4) are very interesting. First, the σ donating capability is very similar for all the olefins studied, with a slight trend favoring the olefins with the *least number of alkyl moieties*. This is counter to the view that alkyl substitution should increase the σ-donating capability of the olefin. The actual trend is a result of the *decrease* in the orbital overlap as the number (and size) of alkyl moieties around the C═C bond increases. This behavior is a result of the repulsive interactions between the alkyl groups and the CO ligands, which force the HOMO of the olefin to be further away from the metal LUMO. The concomitant decrease in orbital overlap negates any increase in the interaction occurring as a consequence of the narrowing of the energy gap that results from an increase in the number of alkyl groups around the C═C bond. The qualitative results from the bonding capability graph correlate well with the changes in the Mulliken population of the olefin HOMO shown in Table 5. The ethylene HOMO donates 0.39 electrons, that is 0.04 to 0.05 more electrons than the HOMO of the monoalkyl and dialkyl substituted ethylenes, and 0.06 more electrons than the HOMO of tetramethylethylene (TME).

In terms of back-bonding, the bonding capability graph (Figure 4) indicates that an increase in the number of alkyl groups around the double *bond decreases the back-bonding capability of the olefin*. This decrease occurs because both the metal HOMO−olefin LUMO energy gap increases *and* the MO overlap decreases. The change in the Mulliken population of the olefin's LUMO (Table 3) correlates well with the trend observed in Figure 4. The population of the ethylene LUMO is 0.27, while the LUMO populations for the monosubstituted olefins are in the range 0.23−0.24, with the exception of DMB (0.19). The LUMO populations for the disubstitued olefin complexes are in the 0.21−0.19 range, and the population of TME's LUMO is 0.15.

TABLE 5: Mulliken Population Changes, Overlap Integrals, and FMO Energy Gaps (eV) for the $Cr(CO)_5$(olefin) Complexes

	Eth	Pro	But	Hex	DMB	c-2-but	t-2-but	isobut	TME
				Olefin Mulliken FMO Population Change					
$-P(L)_\pi$	0.39	0.36	0.36	0.35	0.33	0.35	0.35	0.35	0.33
$P(L)_{\pi^*}$	0.27	0.23	0.24	0.24	0.19	0.2	0.21	0.19	0.15
				HOMO−LUMO Overlap Integral					
$\lvert\langle a\rvert b\rangle\rvert_\sigma$	0.279	0.256	0.257	0.254	0.26	0.238	0.234	0.247	0.216
$\lvert\langle a\rvert b\rangle\rvert_\pi$	0.174	0.162	0.161	0.159	0.141	0.156	0.144	0.146	0.136
				HOMO−LUMO Energy Gaps					
$\Delta E_{gap}\,\sigma$	2.07	1.53	1.55	1.53	1.55	1.09	1.09	1.23	0.572
$\Delta E_{gap}\,\pi$	4.85	5.15	5.12	5.15	5.21	5.42	5.32	5.34	5.56

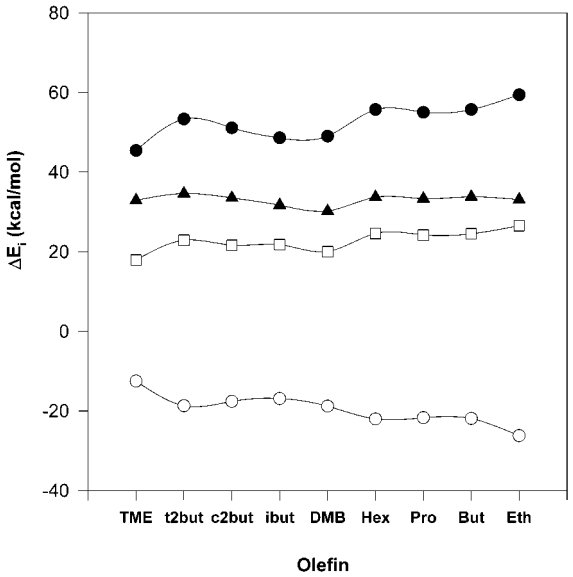

Figure 5. A plot showing the trend in attractive (ΔE_{oi}, ●) and repulsive (ΔE_{ste}, ○) electronic energy for the series of olefin complexes under study. The arithmetic sum of the attractive and repulsive terms yield a net electronic interaction energy (ΔE_{int}, ▲). The calculated bond energy is also shown ($\Delta E = \Delta E_{int} + \Delta E_{def}$, □).

Figure 5 shows the trends obtained for the different energy terms resulting from the bond energy decomposition analysis. The magnitude of *both* the attractive (ΔE_{oi}) and the repulsive (ΔE_{steric}) energy terms decrease as the degree of substitution of the olefin increases. ΔE_{oi} for ethylene interacting with chromium pentacarbonyl is larger than for the substituted olefins. Also, the trend is that the magnitude of the electronic interactions decrease as the extent of the alkyl substitution around the C═C bond increases. Because of its relative size ethylene is expected to have the smallest steric energy. Furthermore, ΔE_{steric} should increase as the size of the olefin increases. The trend in the magnitude of ΔE_{steric} can be rationalized in terms of the size and geometry of the olefin and the metal−olefin distance (in Table 2). Ethylene, which is the smallest of the olefins, can get closer to the metal orbitals than the other olefins, and as a result the ethylene complex has the smallest $Cr-C_{ole}$ bond length. As the size of the olefin increases, the metal−olefin bond length also increases as a result of an increase in the repulsive forces between olefin and metal moiety. As a result, the substituted olefins do not interact with the chromium pentacarbonyl moiety as strongly as ethylene, *and both the attractive and repulsive interactions decrease*.

Figure 5 also shows that there is effectively a balance between the electronic interactions: ΔE_{oi} and ΔE_{steric}. This can be explained qualitatively by the following argument. To increase the orbital interaction energy the olefin must be closer to the metal. However, this results in an increase in the steric energy. The result is that the total electronic interaction energy ($\Delta E_{int} = \Delta E_{oi} + \Delta E_{ste}$) is similar (within ±3 kcal/mol) for all olefins, and that the trend in ΔE is then dominated by differences in the deformation energies for the complexes. (Note that ΔE_{oi} and ΔE_{steric} are calculated for "deformed" fragments.) Figure 5 also shows that that olefins with the same number of alkyl groups have similar interaction energies (ΔE_{oi}). Interestingly, DMB does not fall on the same line as the other monoalkyl ethylene complexes. The interaction of DMB with $Cr(CO)_5$ is weaker than the interaction of propene (Pro), butene (But) and hexene (Hex). As can be inferred from Figure 4, the differences are mainly due to the extent of orbital overlap for the back-bonding interaction. For $Cr(CO)_5$(DMB) the smaller overlap of relevant MOs is principally due to the steric constraint imposed by the bulky *tert*-butyl group. This clearly demonstrates that the size of the alkyl group also effects the bonding interaction.

B. Steric Effects and Deformation Energies. Recent calculations[23,37] for iron and chromium carbonyl-perhalogenated olefin complexes have demonstrated that the deformations taking place in the olefin and in the metal fragment, when they go from their equilibrium ground-state geometries to the geometry they adopt in the complex, involve a significant energy cost (ΔE_{def}). Further, in the perhalogenated olefin−metal complexes that were studied, ΔE_{def} can be a dominant factor in the trend in bond energies. A similar statement can be made for the systems discussed herein: The deformation energy is a critical factor in the trend in BDEs for the complexes studied in this work. The results of the calculation of ΔE_{def} indicate that the total deformation energy (Table 4) is affected by the nature of alkyl group(s) around the C═C bond. For instance, for ethylene ΔE_{def} is 6.7 kcal/mol, for the monoalkyl-ethylenes ΔE_{def} is 9.1 kcal/mol, except for butene where it is 9.3 kcal/mol and for DMB, where it is 10.2 kcal/mol. In the case of the dialkylethylenes, ΔE_{def} ranges from 9.9 kcal/mol in isobutene to 13.0 kcal/mol in *trans*-2-butene. The largest ΔE_{def} is for TME (tetramethylethylene), where it is 15.0 kcal/mol. The total ΔE_{def} can be decomposed into terms corresponding to deformations of the olefin and of $Cr(CO)_5$:

$$\Delta E_{def} = \Delta E_{def}(\text{olefin}) + \Delta E_{def}(Cr(CO)_5) \qquad (10)$$

The results of this partitioning are more revealing than ΔE_{def} itself, as they provide insights into the source of differences in the total ΔE_{def}.

For these complexes the deformation of $Cr(CO)_5$ is affected by the number of alkyl moieties around the double bond: For the $Cr(CO)_5$(ethylene) complex, $\Delta E_{def}(Cr(CO)_5)$ is only 1.1 kcal/mol; for the monoalkylethylenes it is 2.6 kcal/mol (see Table 4), for the dimethylethylenes it is in the range 3.4−3.9 kcal/mol, and for tetramethylethylene $\Delta E_{def}(Cr(CO)_5)$ is 6.2 kcal/mol. The deformation of $Cr(CO)_5$ results principally from the repulsion between the alkyl moieties on the olefin and the CO ligands that are cis and aligned with the C═C bond of the olefin. The CO−alkyl repulsion forces the CO ligands to bend away

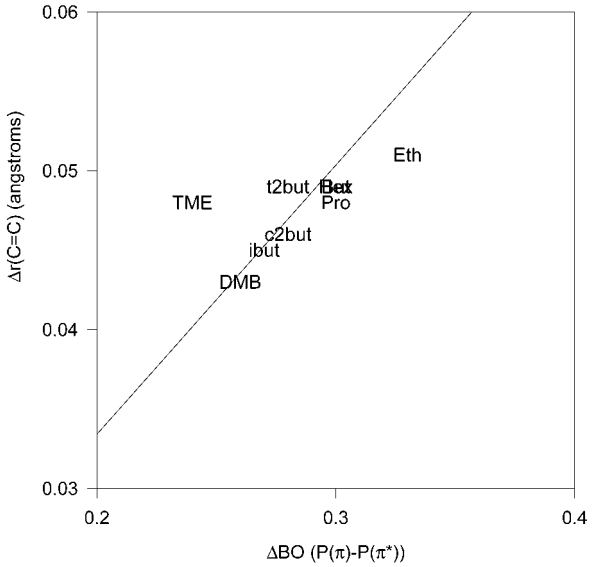

Figure 6. A plot showing the correlation between the calculated changes in C═C bond length and bond order of the complexed olefin. The points for hexene and butene overlap.

from the olefin, as evidenced by the values of the C−Cr−C and Cr−C−O bending angles for CO ligands cis to the olefin (see Table 2 and Chart 1). The CO ligands that are in or close to the plane of the C═C bond bend more than those that are perpendicular to the C═C bond, because they are relatively closer to the olefin.

The olefin also deforms: both as a result of the repulsion between the alkyl groups of the olefin and $Cr(CO)_5$, and as a result of the rehybridization of the olefinic carbons (from sp^2 toward sp^3). The latter effect is a consequence of metal−olefin bonding interactions. Rehybridization of the olefin is evident from the change in the C═C bond length that occurs as a result of complexation. As seen in Figure 6, the C═C bond length change (Δr(C═C)) correlates well with the change in bond order (ΔBO) of the olefin, which is calculated by taking the difference in the populations of the π and π^* MOs of the olefin. The line in Figure 6 is drawn to include the bond order-bond length changes for an sp^2 bond and for complete rehydridization from sp^2 to sp^3 (0.00 Å for no bond order change and 0.2 Å for $\Delta BO = 1$). As can be seen in Figure 6 the extent of rehybridization, though somewhat different for each of the olefins, is similar. Since ethylene has the largest degree of rehybridization it would be expected to have the largest contribution to the olefin deformation energy from this factor. Additionally, since ethylene has the smallest total olefin deformation energy it is then clear that the percentage of the olefin deformation energy due to rehybridization is largest for ethylene.

ΔE_{def}(olefin) values for propene, butene, and hexene are in the 6.5−6.7 kcal/mol range. This means that, relative to C_2H_4, they experience a deformation that involves at least an additional 1.0−1.2 kcal/mol, due to the alkyl CH−CO interaction. DMB, which like propene, butene, and hexene is a monoalkyl ethylene, has a ΔE_{def} of 7.5 kcal/mol. Thus ΔE_{def}(olefin) is at least an additional 2.1 kcal/mol relative to ethylene, and since the degree of rehybridization of DME is less than that for the linear alkenes, ΔE_{def}(olefin) for the $Cr(CO)_5$(DME) complex is at least an additional 1.0 kcal/mol relative to ΔE_{def}(olefin) of the other monoalkyl ethylene complexes. The difference between the value for DMB and the linear olefins is attributable to the *tert*-butyl CCH_3−CO repulsive interactions, which are larger than the CH−CO repulsive interactions for the propene, butene, and hexene complexes. The displacement of the alkyl moieties out of the C═C plane is a manifestation of these repulsive interactions. For example, in the DMB complex the *tert*-butyl group is 16.2° from the C═C plane, while the alkyl substituents in the linear alkenes are ∼14° from this plane. In addition to the bending of the *tert*-butyl group away from the C═C plane, the DMB complex responds to the CO−*tert*-butyl repulsion by a stretching of the Cr−$CHC(CH_3)_3$ bond (2.492 Å), such that the *tert*-butyl−CO distance is larger than the linear alkyl chain−CO distance in the linear monoalkyl ethylenes.

The position of the alkyl groups in the dimethyl-olefins (*cis*- and *trans*-2-butene and isobutene) leads to a different interaction geometry which leads to differences in the ΔE_{def}(olefin) values for these complexes. In *cis*-2-butene, the two methyl groups are cis to each other and trans to the CO ligands. In response to the repulsion from the CO ligands, both methyl groups bend away from the C═C plane. In the *cis*-2-butene complex the angle (Θ) formed between the methyl groups and the C═C plane is 1.1° greater than the corresponding angle between the hydrogens and the C═C plane in the ethylene complex. In addition, the Cr−$CHCH_3$ distance increases by 0.09 Å relative to the Cr−CH_2 distance in the ethylene complex (2.412 Å in the *cis*-2-but complex vs 2.323 Å in the C_2H_4 complex). Isobutene has the methyl groups on the same carbon. Similar to the *cis*-2-butene isomer, both methyl groups move away from the metal fragment by bending of the methyl groups out of the plane of the olefinic bond (0.8° more relative to the hydrogens in ethylene). Additionally, the repulsion between the methyl groups and the equatorial COs in this complex is alleviated by a stretching of the Cr−$C(CH_3)_2$ bond, such that it is 0.12 Å larger (2.532 Å) than the Cr−$CHCH_3$ bond in *cis*-2-butene, and 0.21 Å larger than the Cr−CH_2 bond distance in C_2H_4.

trans-2-Butene shows the largest ΔE_{def}(olefin). The difference relative to *cis*-2-butene is 2.1 kcal/mol, and is caused by the greater bending of the methyl groups away from the C═C plane that results from the $CHCH_3$−CO repulsive interactions. In *trans*-2-butene each methyl group deviates by 18.4° from the C═C plane, compared to 11.7° in *cis*-2-butene. Finally, the most substituted olefin, tetramethylethylene (TME), has a ΔE_{def}(olefin) of 8.8 kcal/mol. The larger ΔE_{def}(olefin) for this complex results from the bending of the methyl groups away from the C═C plane. Each methyl group in TME is bent 14.1°, which is an additional 3.5° with respect to the bending of the hydrogens in the ethylene complex. In addition, the olefin is further away from the metal. The Cr−$C(CH_3)_2$ bond length is 0.17 Å larger than the Cr−CH_2 bond length in $Cr(CO)_5(C_2H_4)$.

Another interesting aspect of the trends in bond energies is the effect of the size of the alkyl group on the BDE. The differences between the linear monoalkyl ethylenes and DMB are significant. The size and geometry of the *tert*-butyl group of DMB contributes to the increment in the repulsive interactions that lead to larger deformations of both the olefin and $Cr(CO)_5$. Interestingly, the differences in the deformation energy among the linear alkenes are not significant, because the alkyl chain can rearrange itself to point away from the metal center so that it does not significantly interact with the cis COs. Thus, the geometry and size of the alkyl substituents situated adjacent to the double bond is a critical factor in determining the deformation energy and it is potentially more important than the length of the olefin chain.

C. Comparisons with Data on Other $Cr(CO)_5$(olefin) Complexes. As previously indicated, McNamara et al.[10] report activation energies for the dissociative loss of olefin from $Cr(CO)_5$(olefin) complexes for a number of olefins ranging from ethylene to 2-methyl-2-butene. These activation energies do not

vary significantly for the olefins studied, and range from 24.0 to 24.8 kcal/mol, with an uncertainty of 0.3−0.4 kcal/mol. However, there are significant differences in the stability of these complexes. They report that these differences in stability are due to differences in the magnitude of the preexponentials for the rate constants for dissociative loss of olefin. These preexponentials vary from 4×10^{16} s^{-1} for ethylene to 6×10^{18} s^{-1} for 2-methyl-2-butene with a reported uncertainty in the 30−50% range. The results reported by McNamara et al. agree well with other results on the dissociative loss of ethylene from $Cr(CO)_5$(ethylene).[30,38]

The activation energy for loss of DMB from $Cr(CO)_5$DMB has been measured in this study as 19.5 ± 1.7 kcal/mol with a preexponential of 1.6×10^{14} s^{-1}. This is a smaller preexponential and activation energy than we would expect based on the trends in the data by McNamara et al. Yang et al.[11] report solution phase data for a number of olefins where the BDEs are also smaller than would anticipated based on the trends in the data in ref 10. The present work and our prior work on iron and chromium olefin complexes demonstrates that substituents on an olefin can have a significant effect on the magnitude of the deformation energy of metal−olefin complexes, which in turn can affect the BDEs of such complexes. The present work indicates that the lower bond energy for the $Cr(CO)_5$(DMB) complex relative to $Cr(CO)_5$ complexes of linear olefins is also a result of the deformations necessary to accommodate binding of DMB. Of course, the activation energy is not the only factor determining the stability of a complex. McNamara finds that the preexponentials for substituted olefins are unusually large due to the entropy change that occurs in going from the energized molecule to the transition state. Both effects could be operative for a given system(s). In addition, in the context of the model in ref 10, it has been pointed out that the differences in *A* factors for the DMB complex versus the linear olefin complexes studied in ref 10 could be a result of differences in their bonding configurations.[39] In the model in ref 10, lower *A* factors would be expected for the $Cr(CO)_5$(DMB) complex if, as a result of its bonding configuration, DMB has more orientational freedom when bound to $Cr(CO)_5$ than the longer chain linear olefins. It would then follow that the minimum energy geometry for this complex may require much less "tightening" of low-frequency vibrations. As a consequence there would be less of an increase in the vibrational state density on dissociation of the DMB complex than would be expected for dissociation of the corresponding complexes of the linear olefins. This would lead to less of a statistical driving force in the exit channel for the unimolecular decomposition of the DMB complex, which would translate to a smaller A factor than measured for the complexes of linear olefins. Further detailed study of these issues would be expected to provide more insights into these differences.

Finally, we note that even though the activation energy for loss of DMB from $Cr(CO)_5$(DMB) is smaller than we would have anticipated based on trends in McNamara's data, the difference between the experimentally determined activation energy reported in this study and 24 kcal/mol (a typical value from McNamara's work) is only approximately 10%, when the error limits on the data reported in this study are taken into account. We also note that there is very good agreement (within the error limits) between the calculated activation energies for loss of olefin from $Cr(CO)_5$(propene) and $Cr(CO)_5$(butene) and that the differences between calculated and measured activation energies for complexes with the isomers of butene are still within ~3 kcal/mol of each other. We therefore conclude that the only significant difference between the experimental activation energy data reported by McNamara et al. and the present calculations is the *trend* in BDEs (or the equivalent activation energies) for the chromium pentacarbonyl complexes involving isomers of butene.

VI. Conclusions

$Cr(CO)_5$(DMB) (DMB = 3,3-dimethyl-1-butene) was generated in the gas phase by addition of DMB to photolytically produced $Cr(CO)_5$. The bimolecular rate constant for this process is $(7.0 \pm 1.5) \times 10^{-11}$ cm^3 $molecule^{-1}$ s^{-1} at 298 K, and is temperature independent within experimental error over the 279−298 K temperature range. The enthalpy for chromium−olefin bond in the $Cr(CO)_5$(DMB) complex has been experimentally determined to be 20.1 ± 1.7 kcal/mol, at 298 K, in the gas phase. The rate constant for dissociative loss of DMB from $Cr(CO)_5$(DMB) has a preexponential given by $\ln A = 32.7 \pm 3.0$.

Chromium−olefin bond energies and enthalpies were calculated using density functional theory (DFT) with a BP86 functional for the complexes $Cr(CO)_5$(olefin) (olefin = ethylene, propene, butene, hexene, DMB, *cis*-2-butene, *trans*-2-butene, isobutene, and tetramethylethylene). Calculated chromium−olefin bond energies for monoalkylethylene (propene, butene, hexene and DMB) complexes are similar, with the exception of DMB, in which the alkyl group is bulkier than in propene, butene and hexene.

DFT-based energy decomposition and Mulliken population analyses were carried out to provide additional insights into the effects of alkyl substitution on the chromium−olefin bond energy for the complexes. The results indicate that an increase in the number of alkyl groups around the C=C bond in these complexes does not increase the σ-bonding interaction between the olefin and the metal centered moiety. This occurs because although the trend is a decrease in the olefin HOMO−metal LUMO energy gap as additional alkyl groups are added to the olefin, there is also a trend of a *decreasing* HOMO−LUMO overlap as a result of repulsive interactions between the alkyl moieties in the olefin and the CO ligands cis to it. This trend of decreasing orbital overlap more than negates the favorable effect of the decrease in the HOMO−LUMO energy gap. For these complexes an increase in the number (and size) of the alkyl moieties around the double bond leads to a *decrease* in the extent of back-bonding because both the metal HOMO−olefin LUMO energies increase and the overlap of the relevant MOs decrease. The size of the substituent can have an effect on the degree of orbital overlap, which affects the σ and π bonding interactions of the olefin. However, an increase in the number and size of the alkyl moieties around the double bond also correlates with a decrease in ΔE_{steric} (see Figure 5), principally due to the fact that additional bulky alkyl groups result in a larger metal−olefin distance. Thus, interestingly, despite the differences in σ and π bonding interactions among all the olefins complexes studied, the values for their net chromium−olefin electronic interaction energies ($\Delta E_{oi} + \Delta E_{steric}$) are very similar: ranging from 30.2 to 34.6 kcal/mol. This implies that the deformation energies associated with the geometrical changes taking place when the olefin and $Cr(CO)_5$ go from their isolated ground-state geometries to the ones they adopt in the complex is a critical factor in the trend in bond energies. The deformation in $Cr(CO)_5$ results from repulsive interactions between the substituents on the olefin and the CO ligands cis to the olefin. For the systems under consideration, the energy required to deform $Cr(CO)_5$ is dependent on the

number and nature of the alkyl moieties around the C═C bond: ranging from 1.1 kcal/mol in ethylene to 6.2 kcal/mol in tetramethylethylene. The olefins deform as a result of the geometry changes associated with both the rehybridization of the olefinic carbons (sp^2 to sp^3-like) associated with the bonding of the olefin to the unsaturated carbonyl complex, and the repulsive interactions between the olefin and the CO ligands. Thus, we conclude that the extent of substitution, and the size and orientation of the alkyl groups around the double bond affect the bond strength in $Cr(CO)_5$(olefin) complexes because both the olefin rehybridization, and the repulsive interactions induced by the substituents on the olefin lead to molecular deformations that involve an "energy cost" that is the deformation energy. Though the magnitude of the deformation energy is not large compared to the orbital interaction energy, the *trend* in the deformation energy is the dominant factor in the *trend* in BDEs in the series of complexes studied, and the calculated trend in BDEs agrees well with most available experimental data. Effectively, the deformation energy negates part of the net electronic binding energy leading to a lower metal−olefin bond energy than would result in the absence of the molecular deformations associated with bonding of the olefin to the metal center. The magnitude of this effect depends on the nature of the bound olefin.

Acknowledgment. We acknowledge the support of this work by the National Science Foundation under grant NSF 97-34891. We thank Professor Ed Grant for discussions relating to the present work and the work in ref 10.

References and Notes

(1) Collman, J. P.; Hegedus, L. S.; Norton, J. R.; Finke, R. G. *Principles and Applications of Organotransition Chemistry*; University Science Books: Mill Valley, CA, 1987.

(2) Crabtree, R. H. *The Organometallic Chemistry of the Transition Metals*; Wiley: New York, 1994; p 107.

(3) Yamamoto, A. *Organotransition Metal Chemistry*; Wiley: New York, 1986.

(4) Parshall, G. W.; Ittel, S. D. *Homogeneous Catalysis*; Wiley: New York, 1992.

(5) Dewar, M. J. S. *Bull. Chem. Soc. Fr.* **1951**, *18*, C79.

(6) Chatt, J.; Duncanson, L. A. *J. Chem. Soc.* **1953**, 2939.

(7) Pruchnick, F. P. *Organometallic Chemistry of the Transition Elements*; Plenum Press: New York, 1990; p 343.

(8) MacPhee, J. A.; Panaye, A.; Dubois, J.-E. *Tetrahedron* **1978**, *34*, 3553.

(9) White, D. P.; Brown, T. L. *Inorg. Chem.* **1995**, *34*, 2718.

(10) McNamara, B.; Towns, M. H.; Grant, E. R. *J. Am. Chem. Soc.* **1995**, *117*, 12254.

(11) Yang, G. K.; Peters, K. S.; Vaida, V. *Chem. Phys. Lett.* **1986**, *125*, 566.

(12) Wang, J.; Weitz, E. *J. Phys. Chem. A* **2001**, *105*, 5410.

(13) Weitz, E. *J. Phys. Chem.* **1994**, *98*, 11256.

(14) Seder, T. A.; Church, S. P.; Weitz, E. *J. Am. Chem. Soc.* **1986**, *108*, 4721.

(15) Ishikawa, Y.; Brown, C. E.; Hackett, P. A.; Rayner, D. M. *J. Phys. Chem.* **1990**, *94*, 2404.

(16) *Jaguar 4.0*; Schrödinger, Inc.: Portland, OR, 1999.

(17) Vosko, S. H.; Wilk, L.; Nusair, M. *Can. J. Phys.* **1980**, *58*, 1200.

(18) Becke, A. D. *Phys. Rev. A* **1988**, *38*, 3098.

(19) (a) Perdew, J. P. *Phys. Rev. B* **1986**, *33*, 8822. (b) Perdew, J. P. *Phys. Rev. B* **1986**, *34*, 7406.

(20) Hay, P. J.; Wadt, W. R. *J. Chem. Phys.* **1985**, *82*, 299.

(21) (a) Ditchfield, R.; Hehre, W. J.; Pople, J. A. *J. Chem. Phys.* **1971**, *54*, 724. (b) Hehre, W. J. Pople, J. A. *J. Chem. Phys.* **1972**, *56*, 4233. (c) Binkley, J. S.; Pople, J. A. *J. Chem. Phys.* **1977**, *66*, 879. (d) Hariharan, P. C.; Pople, J. A. *Theor. Chim. Acta* **1973**, *28*, 213. (e) Hehre, W. J.; Ditchfield, R.; Pople, J. A. *J. Chem. Phys.* **1972**, *56*, 2257. f) Francl, M. M.; Pietro, W. J. Hehre, W. J.; Binkley, J. S.; Gordon, M. S.; DeFrees, D. J.; Pople, J. A. *J. Chem. Phys.* **1982**, *77*, 3654.

(22) Deakyne, C. A.; Liebman, J. F. In *Encyclopedia of Computational Chemistry*; Schleyer, P. v. R., Allinger, N. R., Clark, T., Gasteiger, J., Kollman, P. A., Schaefer, H. F., III., Schreiner, P. R., Eds.; Wiley: Chichester, U.K., 1998; Vol. 2, p 1439.

(23) Cedeño, D. L.; Weitz, E. *J. Phys. Chem. A* **2001**, *105*, 8077.

(24) (a) Amsterdam Density Functional, ADF2000.02, SCM; Vrije Universiteit: Vrije, The Netherlands. (b) Baerends, E. J.; Ellis, D. E.; Ros, P., *Chem. Phys.* **1973**, *2*, 41. (c)Versluis, L.; Ziegler, T. *J. Chem. Phys.* **1988**, *88*, 322. (d) te Velde, G.; Baerends, E. J. *J. Comput. Phys.* **1992**, *99*, 84. (e) Fonseca Guerra, C.; Snijders, J. G.; te Velde, G.; Baerends, E. J. *Theor. Chem. Acc.* **1998**, *99*, 391.

(25) (a) Ziegler, T.; Rauk, A. *Theor. Chim. Acta* 1977, *46*, 1. (b) Ziegler, T.; Rauk, A. *Inorg. Chem.* **1979**, *18*, 1558. (c) Ziegler, T.; Rauk, A. *Inorg. Chem.* **1979**, *18*, 1755.

(26) Bickelhaupt, F. M.; Nibbering, N. M.; van Wezenbeek, E. M.; Baerends, E. J. *J. Phys. Chem.* **1992**, *96*, 4864.

(27) (a) Snijders, G. J.; Baerends, E. J.; Vernooijs, P. *At. Data Nucl. Data Tables* **1982**, *26*, 483. (b)Vernooijs, P.; Snijders, G. J.; Baerends, E. J. *Slater Type Basis Functions for the whole Periodic System*, internal report; Free University of Amsterdam: The Netherlands, 1981.

(28) Krijn, J.; Baerends, E. J. Fit Functions in the HFS-Method. Internal report; Free University of Amsterdam: Amsterdam, The Netherlands, 1984.

(29) Mulliken, R. S. *J. Chem. Phys.* **1955**, *48*, 1833.

(30) Wells, J. R.; House, P. G.; Weitz, E. *J. Phys. Chem.* **1994**, *98*, 8343.

(31) Seder, T. A.; Church, S. P.; Ouderkirk, A. J.; Weitz, E. *J. Am. Chem. Soc.* **1985**, *107*, 1432.

(32) Fletcher, T. R.; Rosenfeld, R. N. *J. Am. Chem. Soc.* **1986**, *108*, 1686.

(33) Kelly, J. M.; Bent, D. V.; Hermann, H.; Schulte-Frohlinde, D.; Koerner von Gustorf, E. J. *J. Organomet. Chem.* **1974**, *69*, 259.

(34) Kelly, J. M.; Long, C.; Bonneau, R. *J. Phys. Chem.* **1983**, *87*, 3344.

(35) Fischer, H.; Hofmann, J. *Chem. Ber.* **1991**, *124*, 981.

(36) See: (a) ref 1, section 3.7; (b) ref 7, p 343.

(37) Cedeño, D. L.; Weitz, E. *J. Am. Chem. Soc.* **2001**, *123*, 12857.

(38) McNamara, B.; Becher, D. M.; Towns, M. H.; Grant, E. R. *J. Phys. Chem.* **1994**, *98*, 4622.

(39) Grant, E. Private communication.